Terahertz quantum cascade lasers with large wall-plug efficiency

Cite as: Appl. Phys. Lett. **90**, 191115 (2007); https://doi.org/10.1063/1.2737129
Submitted: 10 March 2007 • Accepted: 12 April 2007 • Published Online: 09 May 2007

Miriam S. Vitiello, Gaetano Scamarcio, Vincenzo Spagnolo, et al.

Terahertz quantum cascade lasers with large wall-plug efficiency

Miriam S. Vitiello[a] and Gaetano Scamarcio[b]
CNR-INFM Regional Laboratory LIT[3], Università degli Studi di Bari, Via Amendola 173, 70126 Bari, Italy and Dipartimento Interateneo di Fisica "M. Merlin," Università degli Studi di Bari, Via Amendola 173, 70126 Bari, Italy

Vincenzo Spagnolo
CNR-INFM Regional Laboratory LIT[3], Politecnico di Bari, Via Amendola 173, 70126 Bari, Italy and Dipartimento Interateneo di Fisica "M. Merlin," Politecnico di Bari, Via Amendola 173, 70126 Bari, Italy

Sukhdeep S. Dhillon[c] and Carlo Sirtori
Matériaux et Phénomènes Quantique Laboratory, Université Paris 7, Bâtiment Condorcet, 75205 Paris Cedex 13, France

(Received 10 March 2007; accepted 12 April 2007; published online 9 May 2007)

Improved optical power performance of bound-to-continuum quantum-cascade lasers operating at 2.83 THz is reported. Peak optical powers of 100 mW at 4 K and power conversion-efficiencies as high as $\eta_w=(5.5\pm0.4)\%$ in continuous wave at 40 K were measured. The η_w values were assessed via an experimental method based on the analysis of the local lattice temperature as extracted by microprobe photoluminescence versus electrical power. From the measured η_w values they extracted a slope efficiency value 0.41 ± 0.11 W/A. © *2007 American Institute of Physics*.
[DOI: 10.1063/1.2737129]

At the present stage of development of terahertz quantum cascade lasers (QCLs),[1–3] some of the top priorities are increasing the maximum operating temperatures and the optical power. A closely correlated goal is the assessment of the electrical-to-optical power conversion efficiency, the so called wall-plug efficiency (η_w). High power conversion efficiencies are highly desiderable to extend the application field of terahertz QCLs to countermeasures or chemical sensing. Low values $\eta_w \leqslant 2\%$ are typically reported.[2,4] Normally, these values are extracted via the direct measurement of the ratio $\eta_w=P_o/P$ between the emitted optical peak power (P_o) and the total electrical power in the device (P). However, the use of this direct method in terahertz QCLs is affected by the large optical divergence of the optical beam that limits the collection efficiency of the laser beam at values as small as $\eta_c \sim 30\%$. This implies that in general the η_w values reported so far have to be considered as lower limits.

In this letter, we report the demonstration of high power bound-to-continuum QCLs operating at 2.83 THz having large wall-plug efficiency. The latter has been assessed using the shift of microprobe photoluminescence as a thermometric property and studying the dependence of the local lattice heating on the laser facet as a function of the electrical power (P).

Figure 1(a) shows the calculated conduction band structure. A miniband (M_1), 15 meV wide, is used for the depopulation of the lower laser level (1) via e-e scattering, while the upper state (2) is designed to lie in a minigap. The diagonal optical transition $2\rightarrow1$ corresponds to a calculated energy difference $E_{12}=11.1$ meV, with a computed dipole matrix element $z_{12}=9.2$ nm. The quantum design is similar to that reported in Ref. 5.

The $GaAs/Al_{0.15}Ga_{0.85}As$ heterostructures have been grown by molecular beam epitaxy by a commercial provider. A high structural quality and periodicity is verified by x-ray diffraction measurements.[6] The active region includes $N_P=90$ periods for a total thickness of 11.60 μm and is embedded between two GaAs layers. Their thickness/doping values are 80 nm/$n=5\times10^{18}$ cm^{-3} for the upper layer and 600 nm/$n=2\times10^{18}$ cm^{-3} for the lower layer. These layers, together with the active region, the semi-insulating substrate,

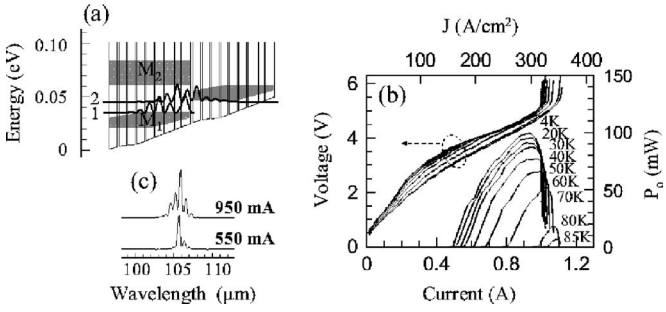

FIG. 1. (a) Conduction band structure of one period of the active region calculated using a self-consistent Schrödinger-Poisson solver with a voltage drop of 27 mV/stage. A 66% conduction band offset is used. Starting from the injection barrier, the layer sequence of one period, in nanometers is (from right to left): **3.9**/14.0/**0.6**/9.1/**0.6**/16.0/**1.5**/12.8/**1.8**/12.2/**2.0**/12.0/**2.0**/11.4/**2.7**/11.3/**3.5**/11.6. AlGaAs layers are shown in bold and the underlined GaAs wells are n doped at 1.6×10^{16} cm^{-3}. The shaded area M_1 represents the lowest energy miniband. M_2 marks the second miniband. The wave function square modulus of the upper and lower laser levels are labeled as 2 and 1, respectively. (b) Voltage and emitted power as a function of current measured at different heat sink temperatures. The laser was driven in pulsed mode, with a 10 kHz repetition rate and a 0.3% duty cycle. This signal was modulated with a 300 Hz square envelope. The optical powers are corrected considering the 0.75 transmittance of the cryostat window. (c) Emission spectra from a 2-mm-long, 150-μm-wide laser device recorded at 4 K for different values of current pulses.

[a]Electronic mail: vitiello@fisica.uniba.it
[b]Electronic mail: scamarcio@fisica.uniba.it
[c]Present address: Laboratoire de Pierre Aigrain Ecole Normale Supérieure, 75231 Paris Cedex 05, France.

and the top contact metallization, form a surface-plasmon waveguide.[7] Laser bars have been fabricated at the clean room of the CNR-INFM Regional Laboratory LIT[3] by optical photolithography. The devices have been wet etched into 150 μm wide and 12 μm deep ridge waveguides. Two bottom contacts are then evaporated on both sides of the stripes (Ni/Ge/Au/Ni/Au:5/12/27/30/300 nm). The top contact is provided by two 12-μm-wide stripes (Ge/Au:6/13 nm) deposited along the edges of the ridge. Each contact has been alloyed at 390 °C for 30 s. A Ni/Au (5/300 nm) not alloyed confining layer is further evaporated completely covering the top of the stripe. The joint use of metal stripes and top not-alloyed contact differs from Ref. 5 and mimics the procedure proposed in Ref. 8 that exploits a trade-off between the increase of top contact series resistance and the decrease of the waveguide losses associated with Ge/Au diffusion during annealing. The substrate was then thinned down to 250 μm and a Ni/Au (5/300 nm) layer deposited as backside metallization.

Laser bars 2 mm long have been cleaved, indium bonded to copper holders, and mounted on the copper cold finger of a helium-flow cryostat (Janis ST300). The heat sink temperature T_{H1} has been controlled with a thermocouple mounted on the cold finger at a distance of about 3 cm from the laser bar. The cryostat output window was a 0.25-mm-thick polypropylene sheet characterized by an ~75% transmissivity at ≈3 THz. The device was biased by applying 300-ns-long pulses at a repetition rate of 10 kHz. This signal was modulated with a 300 Hz square envelope to match the frequency response of the Si bolometer.

Figure 1(b) shows the pulsed current-voltage (*I-V*) and light-current (*L-I*) characteristics measured as a function of the heat sink temperature (T_{H1}) for the investigated device. The threshold current density is $J_{th}=140$ A/cm^2 at 4 K, with a maximum collected peak optical power $P_o=100$ mW and a maximum operating temperature of 85 K in pulsed mode. Note that experimental voltage drop at threshold for alignment at 4 K is ~2.9 V, i.e., ~35% larger than that reported in Ref. 5, probably due to the use of a not-alloyed top contact. We measured a slope efficiency $dP_o/dI=0.40$ W/A at $T_{H1}=4$ K, ~15% higher than that reported in terahertz QCLs fabricated with a high reflectivity coating evaporated on one facet and showing the highest emitted optical power.[3] From the collected P_o and P values we extracted a wall-plug efficiency per facet $\eta_w \approx 2.4\%$ at $T_{H1}=4$ K.

Representative emission spectra are shown in Fig. 1(c). Each spectrum has been collected in rapid-scan mode with a resolution of 0.25 cm^{-1} by using a Fourier-transform interferometer and an $f/2$ off-axis parabolic mirror coated with nickel for light collection. The laser shows a multimode operation with a longitudinal mode spacing $\Delta\nu=0.58$ cm^{-1}.

Figure 2(a) shows the continuous wave (cw), *I-V*, and *L-I* characteristics collected at $T_{H1}=20$ K.[9] A lasing threshold $J_{th}=215$ A/cm^2 and a maximum optical power $P_o \sim 24$ mW have been measured with a calibrated pyroelectric detector. The slope efficiency is $dP_0/dI=0.34$ mW/A. In Fig. 2(b) we show the differential resistance dV/dI as a function of the injected current, measured under the same experimental conditions. The drop at 0.63 A and the negative differential resistance at 1.02 A in Fig. 2(b) mark the lasing range of our device.[10] The measured ratio $P_o/P \sim 0.07$ gives

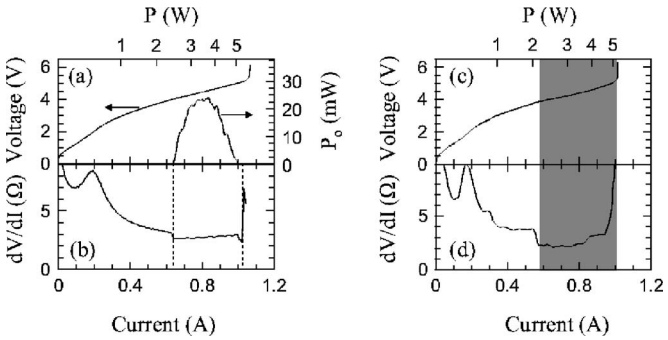

FIG. 2. (a) Voltage vs injected current (*V-I*) and emitted power vs current (*L-I*) characteristics collected at a heat sink temperature $T_{H1}=20$ K, measured 3 cm away from the device in continuous wave (cw). The optical powers are corrected considering the 0.75 transmittance of the cryostat window. (b) Differential resistance vs current characteristics under the same experimental conditions. The dotted vertical lines define the lasing region. (c) cw *I-V* characteristics collected at $T_{H2}=40$ K, measured in close contact with the device and (d) corresponding differential resistance vs current characteristics. The shaded area marks the lasing region.

a lower limit for the total power conversion efficiency $\eta_w > 1.4\%$.

An alternative way to estimate η_w is based on the measurement of the difference $P-P_t=P_o$, where P_t is the thermal power dissipated via Joule heating that can be related with the device thermal resistance (R_L) by the relation $R_L=\Delta T/P_t$. The temperature difference ΔT between the active region and the heat sink can be measured using the microprobe band-to-band photoluminescence technique recently exploited by us to study the thermal properties of QCLs.[11–13] Then, η_w can be obtained using the relation[14] $\Delta T/P=(1-\eta_w)R_L$. We have mounted the QCL on the cold finger of a helium flow microcryostat (Oxford Instruments), in which we simultaneously measured the heat sink temperature (T_{H1}) by using a thermocouple on the cold finger ~4 cm away from the laser bar and the temperature of the device copper mount (T_{H2}) with a calibrated Si diode mounted in close contact with it (see inset of Fig. 3). In our experiments,

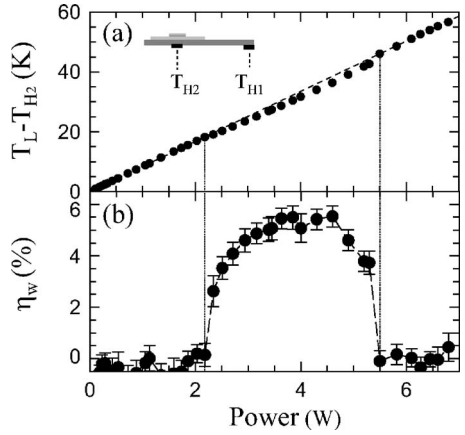

FIG. 3. (a) Difference between the lattice temperature T_L and the temperature of the copper holder T_{H2} plotted as a function of the electrical power (P) in the active region of the device. Inset: schematics of the sample mounting and cryostat cold finger showing the position of the temperature sensors. The slope of the dashed line corresponds to the thermal resistance of the device in the region $P<2.2$ W. (b) Total wall-plug efficiency plotted as a function of P. The dashed line is a guide for the eye. The dotted vertical lines mark the lasing region.

we controlled the He flow in order to keep the device at a fixed T_{H2} while changing P.

Figures 2(c) and 2(d) show the I-V characteristics and the differential resistance measured in cw at $T_{H2}=40$ K. The lasing range, marked by the sudden changes in the differential resistance plot, is within the limits: 198 and 330 A/cm^2. The corresponding cold finger temperatures are $T_{H1}=15$ K and $T_{H1}=5$ K, respectively. Note that both temperatures are lower than the T_{H1} value of Fig. 2(a), thus explaining the lower limits of the lasing range in Fig. 2(c). Under the above experimental condition laser action has been observed up to $T_{H2}=54$ K.

To measure the local lattice temperature, we used the PL peak energy shift as a function of P as a thermometric property, following the method developed by us for the investigation of mid-IR (Ref. 15) and terahertz QCLs.[11,12,16] Figure 3(a) shows the difference ΔT between the temperature measured in the middle of the laser facet and T_{H2} plotted as a function of P. Below the lasing threshold, where $P=P_t$, ΔT increases linearly with P with a slope, coincident with the thermal resistance, $R_L=8.4$ K/W. In the lasing region, the total wall-plug efficiency can be extracted from the data of Fig. 3(a) using Eq. (1), as plotted in Fig. 3(b). The maximum value is $\eta_w=(5.5\pm0.4)\%$. At $P>5.4$ W, beyond the roll-off, ΔT increases linearly with P with the same slope R_L measured below threshold.

The measured wall-plug efficiency can be used to extract the total slope efficiency at threshold of the investigated QCLs, using the relation $\eta_w=2(dP_o/dI)(1/V-\Delta V)(1-(I_{th}/I))$, where $V-\Delta V$ is the applied voltage on the active region, calculated by subtracting the parasitic drop $\Delta V \sim 0.6$ V. At $P=2.94$ W ($I=0.71$ A), we found the value $dP_o/dI=0.41\pm0.11$ W/A. This value is a factor of ~ 1.2 larger that extracted from the L-I characteristics of Fig. 2(a), due to the lower operating temperature, as confirmed also from the drop in the differential resistance at threshold that is a function of the upper and lower laser level lifetimes.[10] The size of this drop is a factor of ~ 3 larger than in Fig. 2(c). From the measured dP_o/dI value we estimated a differential quantum efficiency of ~ 34 photons for injected electrons at 40 K.

Comparison of the above slope efficiency value with the relation $dP_o/dI=(1/2)N_P(h\nu/q_0)(\alpha_m/(\alpha_m+\alpha_w))\tau$, gives $(\alpha_m/(\alpha_m+\alpha_w))\tau=0.77\pm0.21$, to be considered as a benchmark for the gain modelling of our device. In the previous expressions $\tau=\eta_i[1-(\tau_1/\tau_2)((1/\eta_i)-1)-(\tau_1/\tau_{21})](\tau_2/(\tau_1+\tau_2[1-(\tau_1/\tau_{21})]))$, τ_1 is the lifetime of the lower laser level, τ_2 is the lifetime of the upper laser level, τ_{21} is the scattering time of electrons from level 2 to 1, $h\nu$ is the photon energy, q_0 the electronic charge, and α_m and α_w the out-coupling and waveguide losses, respectively. As a rough estimate, assuming $\tau_1 \ll \tau_2, \tau_{12}$, as confirmed by the differential resistance discontinuity of Fig. 2(d), α_w in the range of 2–5 cm^{-1} and using $\alpha_m=5.85\pm0.10$ cm^{-1} (Ref. 17) our findings suggests an injection efficiency $\eta_i>0.75$ in the investigated device. Such a high η_i value is typical of bound-to-continuum terahertz structures.

CNR-INFM LIT[3] acknowledges partial financial support from MIUR (DD 1105/2002). M.S.V., G.S., and V.S. would like to acknowledge B. Williams, J. Faist, and S. Barbieri for helpful discussions and S. Dhillon and C. Sirtori for their help in the THz optical characterization.

[1] B. S. Williams, S. Kumar, Q. Hu, and J. L. Reno, Opt. Express **13**, 3331 (2005).
[2] C. Walther, G. Scalari, J. Faist, H. Beere, and D. Ritchie, Appl. Phys. Lett. **89**, 231121 (2006).
[3] B. S. Williams, S. Kumar, Q. Hu, and J. L. Reno, Electron. Lett. **42**, 89 (2006).
[4] J. Alton, S. Barbieri, C. Worrall, M. Houghton, H. E. Beere, E. H. Linfield, and D. A. Ritchie, Proc. SPIE **5727**, 65 (2005).
[5] S. Barbieri, J. Alton, H. E. Beere, J. Fowler, E. H. Linfield, and D. A. Ritchie, Appl. Phys. Lett. **85**, 1674 (2004).
[6] M. S. Vitiello, G. Scamarcio, and V. Spagnolo, Proc. SPIE **6485**, 68 (2007).
[7] R. Köhler, A. Tredicucci, F. Beltram, H. E. Beere, E. H. Linfield, A. G. Davies, D. A. Ritche, R. C. Iotti, and F. Rossi, Nature (London) **417**, 156 (2002).
[8] L. Ajili, G. Scalari, D. Hofstetter, M. Beck, J. Faist, H. Beere, G. Davies, E. Linfield, and D. Ritchie, Electron. Lett. **38**, 1675 (2002).
[9] Note that being T_{H1} measured 3 cm far from the device holder, larger temperatures are established during cw operation in the copper mount.
[10] C. Sirtori, F. Capasso, J. Faist, A. L. Hutchinson, D. L. Sivco, and A. Y. Cho, IEEE J. Quantum Electron. **34**, 1722 (1998).
[11] M. S. Vitiello, G. Scamarcio, V. Spagnolo, J. Alton, S. Barbieri, C. Worral, H. E. Beere, D. A. Ritchie, and C. Sirtori, Appl. Phys. Lett. **89**, 021111 (2006).
[12] M. S. Vitiello, G. Scamarcio, V. Spagnolo, B. S. Williams, S. Kumar, Q. Hu, and J. L. Reno, Appl. Phys. Lett. **86**, 111115 (2005).
[13] PL spectra have been obtained by focusing the 647 line of a Kr^+ laser down to a 2.5 μm spot, directly onto the laser front facet using an incident optical power density of $\approx$200 W/cm^2. The low value of the optical pumping power allows us to maintain the electronic distribution unperturbed only providing holes for band-to-band radiative recombination.
[14] J. Vurgaftman and J. R. Meyer, J. Appl. Phys. **99**, 123108 (2006).
[15] V. Spagnolo, G. Scamarcio, D. Marano, M. Troccoli, F. Capasso, C. Gmachl, A. M. Sergent, A. L. Hutchinson, D. L. Sivco, A. Y. Cho, H. Page, C. Becker, and C. Sirtori, IEE Proc.: Optoelectron. **150**, 298 (2003).
[16] M. S. Vitiello, G. Scamarcio, V. Spagnolo, T. Losco, R. P. Green, A. Tredicucci, H. E. Beere, and D. A. Ritchie, Appl. Phys. Lett. **88**, 241109 (2006).
[17] S. Kohen, B. S. Williams, and Q. Hu, J. Appl. Phys. **97**, 053106 (2005).